Article:
Ochs, O., Martsinovich, N., Heckl, W.M. et al. (2020) Quantifying the ultraslow desorption kinetics of 2,6-naphthalenedicarboxylic acid monolayers at liquid–solid interfaces. The Journal of Physical Chemistry Letters, 11 (17). pp. 7320-7326. ISSN: 1948-7185

https://doi.org/10.1021/acs.jpclett.0c01882

Quantifying the ultra-slow desorption kinetics of 2,6-napthalenedicarboxylic acid monolayers at liquid-solid interfaces

Oliver Ochs[1,2], Natalia Martsinovich[3], Wolfgang M. Heckl[1,2], and Markus Lackinger[1,2,]*

[1] Department of Physics, Technische Universität München, James-Franck-Str. 1, 85748 Garching, Germany

[2] Deutsches Museum, Museumsinsel 1, 80538 Munich, Germany

[3] Department of Chemistry, University of Sheffield, Sheffield S3 7HF, UK;

Corresponding Author

*markus@lackinger.org

Abstract

Kinetic effects in monolayer self-assembly at liquid-solid interfaces are not well explored, but can provide unique insights. We use variable-temperature Scanning-Tunneling-Microscopy (STM) for quantifying the desorption kinetics of 2,6-naphthalenedicarboxylic acid (NDA) monolayers at nonanoic acid-graphite interfaces. Quantitative tracking of the decline of molecular coverages by STM between 57.5 °C and 65.0 °C unveiled single exponential decays

over the course of days. An Arrhenius plot of rate constants derived from fits results in a surprisingly high energy barrier of +208 kJ mol^{-1} that strongly contrasts with the desorption energy of +16.4 kJ mol^{-1} with respect to solution as determined from a Born-Haber cycle. This vast discrepancy indicates a high energy transition state. Expanding these studies to further systems is the key to pinpoint the molecular origin of the remarkably large NDA desorption barrier.

TOC GRAPHICS

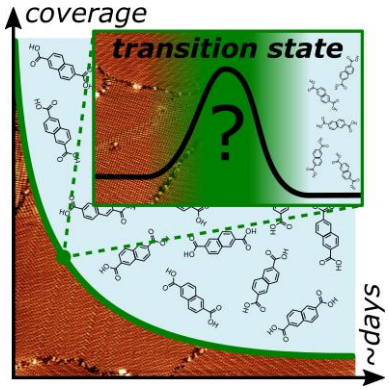

Equilibria are characterized and maintained by the equality of forward and backward reactions. Consequently, attainment of thermodynamic equilibrium necessarily requires a dynamic equilibrium, and hindering of either forward or backward reaction inevitably results in kinetic trapping. Here, we focus on kinetic effects in monolayer self-assembly at liquid-solid interfaces. According to a common assumption, interfacial supramolecular monolayers readily attain thermodynamic equilibrium through continuous exchange of molecules with the supernatant solution. This view is corroborated by observed dynamic responses of monolayers to changes in solution composition or temperature,[1-4] indicating fulfillment of the necessary precondition for applying thermodynamical models. Desorption becomes feasible already at room temperature, because solvation can drastically reduce desorption energies.[5, 6] Hence, the energetics at liquid-

solid interfaces is very distinct from vacuum-solid interfaces, where desorption energies >150 kJ mol^{-1} that prohibit room temperature desorption are common even for smaller molecules. Yet, observations of kinetically trapped phases at liquid-solid interfaces,[7-9] in particular for larger molecules, cast doubt on the prevalent concept of an effective dynamic equilibrium. This view gains support from recent studies that unveiled surprisingly large desorption barriers for porphyrins at liquid-solid interfaces.[10, 11]

Kinetic effects are presently not well explored in monolayer self-assembly at liquid-solid interfaces. Most current studies employ Scanning-Tunneling-Microscopy (STM) which facilitates straightforward assessment of structures in submolecular detail, but lacks sufficient temporal resolution. Only in a few cases, kinetic phenomena with time constants ranging from milliseconds to minutes were studied by STM.[12-15] To nevertheless use STM for quantitative kinetic studies, model systems with exceedingly slow kinetics are desirable. In this respect, variable-temperature experiments allow matching of time constants, because most rate-determining elementary processes are thermally activated, and their rate constants vary strongly with temperature according to the Arrhenius equation. Since the self-assembly process is still too rapid to be captured by STM, we propose to study monolayer dissolution kinetics by tracking surface coverage over time. A closely related process of dissolution kinetics from molecular crystals into (aqueous) solutions also plays an important role in pharmaceutics, because it determines drug dosage rates.[16-19]

We study the dissolution kinetics of 2,6-naphthalenedicarboxylic acid (NDA, Figure 1a) monolayers at the nonanoic acid (9A)-graphite interface. This choice was motivated by previous results that indicated kinetic hindering: NDA monolayers feature uncommonly large defect

densities,[20] whereas comparable dicarboxylic acids self-assemble into highly ordered monolayers.[5, 21, 22]

In the experiments, temperatures are increased until NDA monolayers reach the verge of thermodynamic stability, as indicated by the decline of molecular coverages from typically full at room temperature to partial at elevated temperatures. Thereafter the temporal evolution of molecular coverage is quantitatively tracked over time at constant temperature by real space imaging. Key to these novel experiments is our recently developed Immersion-Scanning-Tunneling-Microscope (I-STM), devised for long-term variable-temperature experiments at liquid-solid interfaces.[23] In most previously reported variable-temperature studies only samples were heated,[3, 24-27] whereby solvent evaporation is unavoidable and can become limiting. We completely removed this crucial limitation by integrating the STM body into a hermetically sealed and precisely temperature-controlled container, a concept similarly implemented by the Hipps group.[28] Thereby long-term variable-temperature STM experiments with unprecedentedly high resolution and low drift become feasible, yet without any principal limitation for the duration of experiments.

STM images of self-assembled NDA monolayers acquired at the 9A-graphite interface are presented in Figure 1. In the ordered domains an oblique unit cell can be assigned with experimental lattice parameters a = (1.16 ± 0.02) nm, b = (0.74 ± 0.02) nm and $\gamma = 56° \pm 1.0°$ Analogous to comparable dicarboxylic acids,[5, 6, 20, 29-32] the NDA monolayer consists of densely packed molecular chains formed by $R_2^2(8)$ H-bonds between the carboxylic acid groups. Pinpointing individual NDA molecules by their STM appearance is not obvious. Yet, Molecular Mechanics (MM) calculations yield a repeat distance of 1.15 nm along the H-bonded chains (Supporting Information, Fig. S10). Precisely the same distance was identified in the STM

images, allowing to elucidate the orientation of the H-bonded chains, and hence that of NDA molecules. Overlaying STM images with the MM simulated chains results in a C-H•••O distance of ~0.24 nm between NDA molecules in adjacent chains, indicating formation of interchain H-bonds.[20, 33]

At room temperature the surface is completely covered with NDA domains extending up to ~300 nm, but smaller domains in the size range (50...100) nm are frequently observed. More importantly, NDA monolayers exhibit an uncommonly low degree of structural perfection. Molecular vacancies are often observed zero dimensional defects (see Figures 1a and b). A frequently observed line-defect is shown in Figures 1b and c. As illustrated by the overlay and corresponding model, it consists of two intermingled H-bonded NDA chains with a chirality opposite to both adjacent domains. These 1D defects persist even at elevated temperatures of 70 °C and are not eliminated by self-healing.

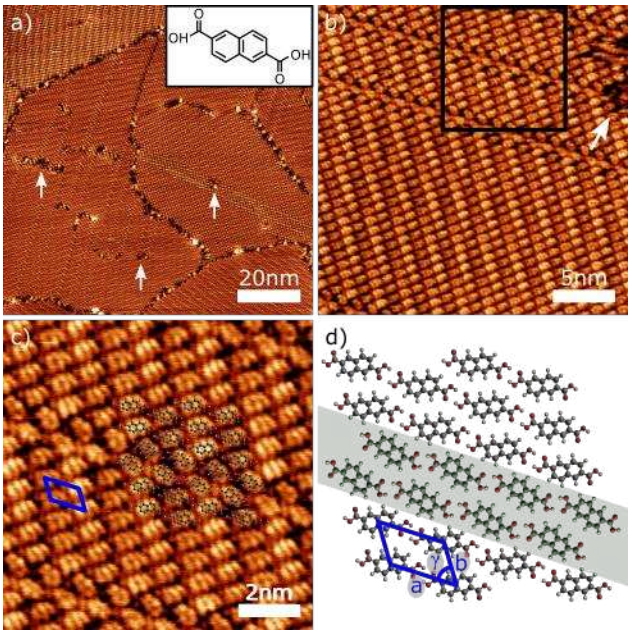

Figure 1. Self-assembly of NDA monolayers at the 9A-graphite interface. STM images were acquired at 70 °C using room temperature saturated solution. **(a)** Large scale STM image

showing multiple domains (insert: molecular structure of NDA). Dark appearing patches within the domains (highlighted by arrows) correspond to vacancies. **(b)** STM image showing a frequently observed line-defect, i.e. an anti-phase domain boundary, demarcated by two H-bonded NDA chains of opposite chirality. **(c)** close up of the area indicated in (b) showing the detailed molecular arrangement. **(d)** Molecular model as derived from (c) and indicated unit cell (image size and tunneling parameters: (a) 100 nm, 0.59 V, 60 pA; (b) 25 nm, 0.27 V, 50 pA; (c) 10 nm, 0.27 V, 50 pA;).

To evaluate the desorption kinetics of NDA monolayers, we studied the temperature evolution of molecular coverages in variable-temperature STM experiments. Upon heating above ~50 °C we observed partial coverages due to desorption of molecules, driven by the thermodynamic instability of full coverages. The pivotal question, however, is whether the observed partial coverages already represent a new stationary state, i.e. a thermodynamic equilibrium partly shifted to the dissolved state, or further decline over time. To address this crucial point, we monitored the surface coverage at constant temperature over time. Coverages were quantified at discrete times by acquiring statistically significant STM data from a surface area of ~3.5 μm² (Supporting Information, experimental methods, Figs. S7 and S8). We measured desorption traces for temperatures between 57.5 °C and 65.0 °C, the results are summarized in Figure 2a. For the lowest measured temperature of 57.5 °C we find a progressively declining coverage over the course of eight days. Note that such long-term experiments were only possible, because solvent evaporation is ceased in the hermetically sealed I-STM.[23] For all traces the data points are well described by single exponential decays, indicating first order desorption kinetics, and allowing to deduce rate constants from fits. For the three lower temperatures improved fits were

obtained by exponential decays to asymptotically reached finite final coverages θ_∞ rather than zero:

$$\theta(t) = \theta_{t=0} \cdot e^{-k \cdot t} + \theta_\infty$$

(e.g. for 57.5 °C R^2 (θ_∞=0 %) = 0.982 *vs.* R^2 (θ_∞=25.8 %) = 0.996). The fitting results are summarized in Table 1. θ_∞ decrease for increasing temperature, with θ_∞=0 actually measured for the highest temperature of 65.0 °C. This behavior is consistent with interpreting θ_∞ as partial coverages in thermodynamical equilibrium. With increasing temperature the thermodynamic equilibrium becomes gradually shifted to lower coverages, because of the growing favorable entropy contribution to the free energy of the dissolved state.

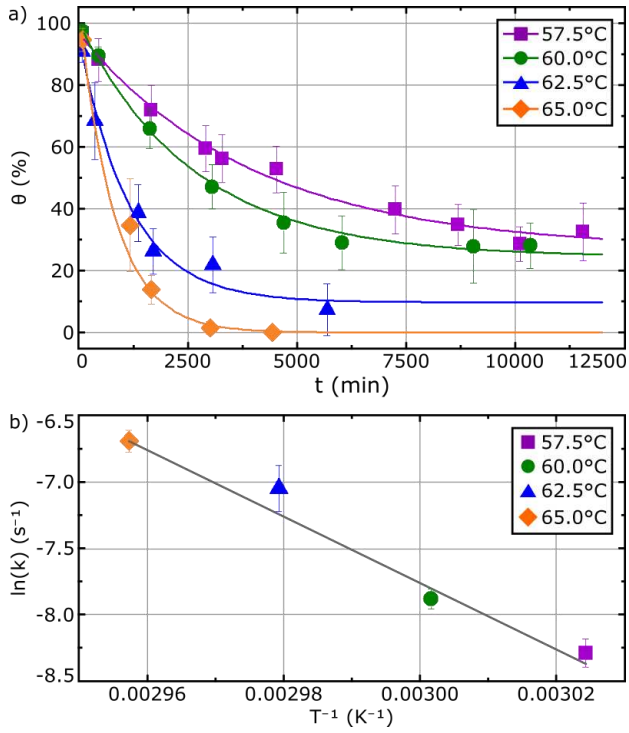

Figure 2. Summarized results of kinetic measurements on NDA monolayer desorption; **(a)** Molecular coverage θ vs. time t traces measured by STM at fixed temperatures (purple squares: 57.5 °C; green dots: 60.0 °C; blue triangles: 62.5 °C; orange diamonds: 65.0°C); Vertical error bars correspond to standard deviations, and (invisibly small) horizontal error bars reflect the

measurement duration of ~90 min. Solid lines represent fits with single exponential decays to asymptotically reached final coverages θ_∞ (cf. Table 1 for fitting results). **(b)** Arrhenius plot of the rate constants. The solid line represents a linear fit, with a slope corresponding to an activation energy of +208 kJ mol^{-1}. Fitting uncertainties account for vertical error bars.

Activation energies of thermally driven processes can be assessed from the temperature dependence of rate constants, with several studies demonstrating the utility of STM experiments.[34-36] All four rate constants derived from fitting desorption traces lie on a straight line in the Arrhenius plot shown in Figure 2b, and the slope of the linear fit corresponds to an activation energy of +208 kJ mol^{-1}. For comparison, fitting the desorption traces of Fig. 2a with single exponentials (i.e. without considering finite θ_∞) would result in a significantly larger desorption barrier of +289 kJ mol^{-1} (Supporting Information, Fig. S9). Hence, considering base values from thermodynamically stable partial coverages is important. Even though relatively high, a desorption barrier of +208 kJ mol^{-1} appears consistent with the ultra-slow kinetics. Remarkably, the NDA desorption barrier is significantly larger than the barriers in the order of (100…150) kJ mol^{-1} deduced for desorption of porphyrins from monolayers into solution based on room temperature STM analysis after quenching from higher temperatures.[10, 11, 37]

Table 1. Rate constants k and asymptotically reached final coverages θ_∞ as obtained from fitting desorption traces acquired at temperatures T; fitting uncertainties are stated in parenthesis;

T (°C)	k (10^{-4} min^{-1})	θ_∞ (%)
57.5	2.51 (±0.26)	25.8 (±2.74)
60.0	3.77 (±0.28)	24.4 (±2.09)
62.5	8.70 (±1.49)	9.80 (±4.52)

65.0	12.4 (±1.04)	0.0

Interpreting and explaining the experimentally derived desorption barrier is essential for a fundamental understanding. The most straightforward assumption is that desorption barriers are equal to desorption energies, i.e. the (free) energy difference between desorbed and adsorbed state of a molecule, in the end implying the absence of a transition state. However, various studies propose sizable barriers for both adsorption and desorption at liquid-solid interfaces associated with solvent rearrangement processes.[38, 39] In the following, we will focus on the energetics of desorption and discuss potential entropy effects later.

We obtained theoretical estimates for NDA desorption energies from MM calculations (Supporting Information, computational methods). Monolayer dissolution is expected to proceed *via* desorption of more weakly bound undercoordinated molecules, e.g. at domain edges. To assess their diminished desorption energies, and also the dependence on the local binding, finite islands of 5×5 molecules were calculated on graphite, results are summarized in Figure 3.

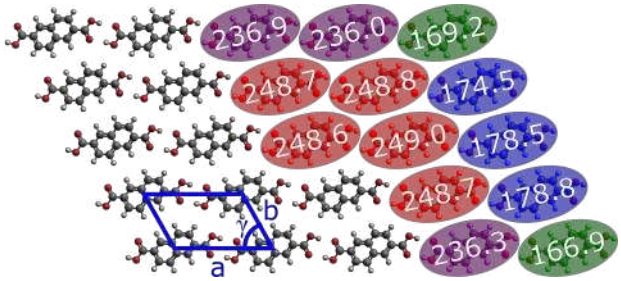

Figure 3. MM calculated desorption energies of NDA molecules (in kJ mol^{-1}) from a finite island of 5×5 molecules. Calculations were conducted on graphite(0001) (not shown for clarity). Depending on the position of the respective molecule in the island and the intermolecular binding to neighbour molecules, desorption energies exhibit sizable spatial variations with the

highest values in the domain interior, and signficant differences between the two inequivalent edges.

In the interior of the domain, NDA desorption energies are essentially constant at ~249 kJ mol^{-1}, whereas notable differences occur between the two inequivalent edges. These can be attributed to differences in H-bonding: Desorption energies are significantly lower at the edge running parallel to the $\vec{b}$ lattice vector, where NDA molecules form H-bonds with only one carboxylic acid group, while the other carboxylic acid group is dangling at the boundary. In contrast, at the edges running parallel to the $\vec{a}$ lattice vector NDA molecules form H-bonds with both of their carboxylic acid groups, and their desorption energy reaches almost that of interior molecules. The small difference of ~12 kJ mol^{-1} can be attributed to the lack of interchain bonding at one side. The desorption energy difference of ~60 kJ mol^{-1} for NDA molecules in the two non-equivalent edges largely reflects the binding energy of $R_2^2(8)$ H-bonds between two carboxylic acid groups.[40, 41] Corner molecules exhibit the smallest desorption energy due to their inferior interaction with neighbors. These results mirror our previous calculations of terephthalic acid which self-assembles into isostructural monolayers on graphite.[42] Furthermore, the outcome is virtually independent of island size. Results obtained for a 3×3 island are essentially similar (Supporting Information, Fig. S12), indicating that diminished desorption energies only occur for molecules directly at the domain edge.

Dissolution and desorption are anticipated to start at and proceed from domain edges, because of the lower desorption energy of these undercoordinated molecules. Moreover, edge sites are not annihilated during the dissolution, hence available for driving it to completion. This is corroborated by STM imaging, where comparatively small NDA domains were observed throughout the monolayer dissolution that constantly provide edge molecules (Supporting

Information, Fig. S8). Yet, high stability of the edges parallel to the $\vec{a}$ lattice vector, and the resulting preferential desorption from edges parallel to the $\vec{b}$ lattice vector should lead to distinct shapes of NDA domains with two parallel and fairly straight edges. However, in STM images we observe rugged domains (Supporting Information, Fig. S8), possibly hinting toward a two-step desorption process: First, NDA molecules detach from the islands, but still remain adsorbed on the graphite surface in a mobile 2D molecular gas phase. Only in the second step, molecules eventually desorb from the graphite surface into solution. This two-step process should be energetically more favourable, but it is not necessarily the dominating process as it could be associated with significantly lower pre-exponentials.

Based on the MM calculations we propose an average desorption energy of edge molecules in the order of +170 kJ mol^{-1}. At first sight, the MM derived NDA desorption energy appears comparable with the activation energy extracted from the Arrhenius plot. Yet, at liquid-solid interfaces NDA molecules desorb into solution, whereas isolated molecules in vacuum were used as reference for MM. Consequently, actual desorption energies are expected to be significantly lowered by solvation and the associated enthalpic stabilization in solution.

In order to estimate enthalpy differences of molecules at liquid-solid interfaces with respect to solution, i.e. to quantify the influence of the supernatant solution, we proposed an adapted Born-Haber cycle.[5] It was originally devised for thermodynamic models, but is similarly applicable to kinetic models.

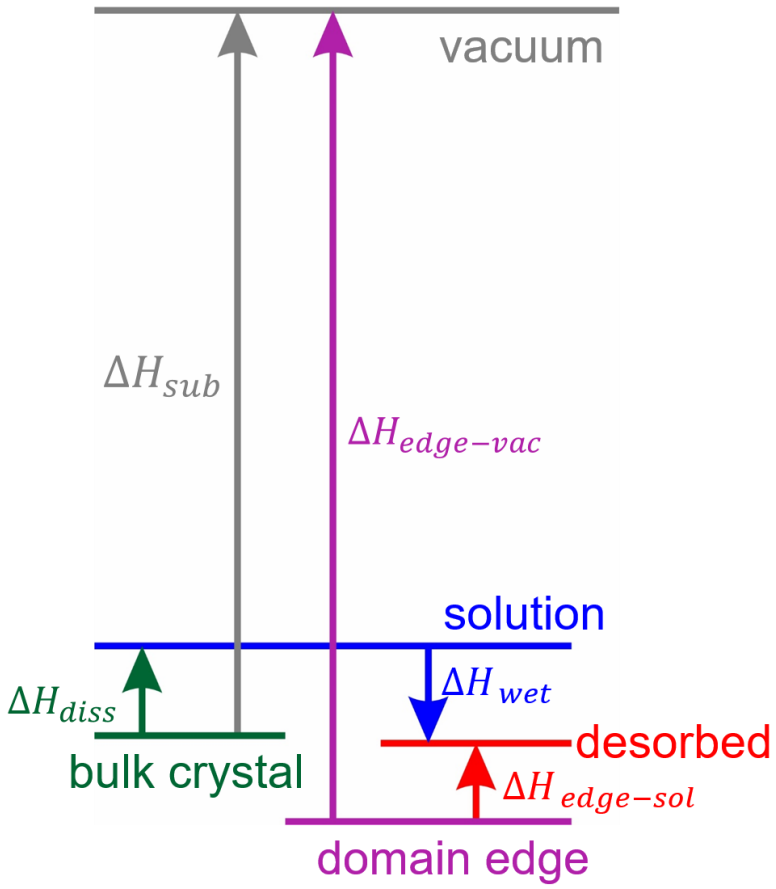

Scheme 1. Born-Haber cycle using single NDA molecules in vacuum, molecules at domain edges, dissolved molecules in solution and the NDA bulk crystal as reference states and considering a wetting enthalpy. Respective enthalpy differences are indicated. The diagram is drawn to scale to illustrate the significant lowering of the desorption energy by the presence of solution.

Its main idea is to introduce the crystalline bulk of solute molecules as additional reference state. According to Scheme 1, the desorption energy (negative binding energy) $\Delta H_{edge-sol} = -\Delta H_{sol-edge}$ of NDA molecules at domain edges with respect to solution is given by:

$$\Delta H_{edge-sol} = \Delta H_{edge-vac} - \Delta H_{sub} + \Delta H_{diss} + \Delta H_{wet}$$

ΔH_{diss} and ΔH_{sub} correspond to NDA dissolution and sublimation enthalpies, respectively, and are both experimentally accessible (*vide infra*). $\Delta H_{edge-vac}$ represents the MM calculated desorption energy of edge molecules into vacuum. ΔH_{wet} considers solvent wetting effects, where upon NDA desorption solution-monolayer interface is exchanged for solution-substrate interface. Since the interaction of solvent molecules with the bare surface is normally stronger than with the monolayer, ΔH_{wet} is often exothermic for desorption.[5, 11]

Temperature dependent measurements of NDA effusion rates in high vacuum yield $\Delta H_{sub} = 152\ kJ\ mol^{-1}$ (Supporting Information, Figs. S1 and S2) in reasonable agreement with the MM calculated bulk binding energy of $143\ kJ\ mol^{-1}$. ΔH_{diss} was determined by measuring the temperature dependence of NDA solubility in 9A by UV-vis absorption spectroscopy (Supporting Information, Figs. S3 and S4). The acquired endothermic $\Delta H_{diss} = +18.8\ kJ\ mol^{-1}$ is in the typical range for comparable solutions.[5] Quantifying ΔH_{wet} is more intricate, but its effect is also often relatively small. We estimate ΔH_{wet} by calculating the differences in adsorption energies of a single 9A molecule on a NDA monolayer *versus* graphite (Supporting Information, calculation methods). We find that adsorption of 9A on graphite is on average ~20 kJ mol^{-1} more favorable as compared to the NDA monolayer. Renormalization to the NDA footprint area results in an exothermic $\Delta H_{wet} = -20.4\ kJ\ mol^{-1}$. Combining all individual enthalpies in the Born-Haber cycle eventually results in a desorption energy for edge molecules into solution of $\Delta H_{edge-sol} = +16.4\ kJ\ mol^{-1}$, in vast discrepancy with the activation energy of $+208\ kJ\ mol^{-1}$ as derived from the Arrhenius plot.

The discrepancy between the two independent approaches is remarkably large. Admittedly, experimental errors in the Born-Haber cycle could also be relatively large, because each individual contribution, notably ΔH_{wet}, bears comparatively large uncertainties that add up in the

error propagation. Nevertheless, the vast discrepancy is too large to be attributed to experimental errors. It rather challenges the common assumption that activation barriers and desorption energies are equal for NDA monolayers at the 9A-graphite interface. This implies a different origin of the desorption barrier, associated with the existence of a high energy transition state. The molecular origin of this transition state remains unknown, however, additional experiments hint toward an important role of solvent composition.

In repeat experiments with 9A solvent from a different batch we find substantial deviations. Remeasuring a desorption trace at 62.5 °C resulted likewise in a single exponential decay, yet the rate constant was ~4.6 times lower, i.e. 1.9×10^{-4} min^{-1} (repeat) as compared to 8.7×10^{-4} min^{-1} (original) (Supporting Information, Fig. S5). Yet, an additional feature in UV-vis absorption spectra of the solvent of the repeat experiment indicated its impurity (Supporting Information, Fig. S6).[43] Its chemical nature remains presently unclear, but we hypothesize that the impurity may be related to chemical changes of the solvent, rather than being a foreign species. Although the difference in rate constants appears rather drastic, it converts into a comparatively small energetic effect, where the desorption barrier is increased by only 4.3 kJ mol^{-1} (assuming similar pre-exponentials).

In summary, we have quantified the activation energy for NDA desorption from monolayers at 9A-graphite interfaces by quantitatively tracking the decline of molecular coverages over time at constant elevated temperatures. NDA desorption proceeds remarkably slow over the course of days. On the one hand, this facilitates quantification by relatively slow *in situ* STM measurements (~90 min to acquire statistically significant data). On the other hand, experiments at fixed elevated temperatures last for up to 8 days. This unprecedented experimental duration for variable-temperature STM experiments at liquid-solid interfaces could only be realized with

our dedicated instrument.[23] Over the measured temperature range from 57.5 °C to 65.0 °C, coverages follow single exponential decays down to a base value θ_∞ that is determined by the temperature dependent position of the thermodynamic equilibrium. The extracted rate constants consistently lie on a straight line in an Arrhenius plot, indicating a constant activation energy for the rate-limiting elementary process. In addition, we quantified the desorption energy with respect to solution using a Born-Haber cycle, suggesting that the presence of solution lowers the desorption energy of +170 kJ mol^{-1} with respect to vacuum down to +16.4 kJ mol^{-1} with respect to solution. The present work focusses on the energetics of desorption, but including entropy contributions, i.e. considering free energies, would be more appropriate. Entropy is the thermodynamic driving force for desorption, and manifests itself in the decreasing equilibrium coverages for increasing temperatures. Yet, the relatively large errors in θ_∞ due to the indirect determination from fits prohibit a detailed analysis.

The key result is that the activation energy as derived from kinetic measurements differs notably from the desorption energy. From this vast discrepancy we conclude on a high energy transition state. However, also here entropic effects are vitally important, because rates are also determined by the free energy of the transition state. High transition state entropies can promote processes with large transition state energies through a large pre-exponential. Currently, we can only speculate about the origin and nature of this transition state. However, assuming a transition state where partly desorbed NDA molecules already gain entropy through leaving the surface, but are not yet energetically stabilized by solvation could explain both a high transition state energy and entropy.

Control experiments show sizeable deviations in rate constants for solvents from two different batches, where differences in the respective UV-vis absorption spectra indicate the presence of

chemically distinct species in one solvent. From this, we hypothesize that the desorption kinetics, but less so the energetics, from NDA monolayers may be strongly influenced by an interfacial boundary layer between adsorbed monolayer and bulk solution. This boundary layer could be rate-determining for desorption, for instance by preventing effective solvation of the desorbing species, as the most important processes for lowering desorption energies.

Fundamental insights are expected from expanding these studies to comparable model systems, i.e. carboxylic acid tectons in fatty acid solvents, for which we recently reported an example of a dynamic structural response already at room temperature without measurable kinetic limitations.[1] Hence, it would be rewarding to explore whether NDA is a singular example for the observed ultra-slow desorption kinetics, and to unveil the underlying reasons at the molecular level. The first hint toward kinetic hindering that also originally motivated this study on NDA desorption was the low structural quality of its self-assembled monolayers, which is an exception rather than the rule. In the light of inhibited desorption, the persistence of the frequently observed line-defects (Figure 1) at higher temperature is particularly interesting as it suggests an important role of desorption-readsorption processes for self-healing, in particular for prochiral NDA molecules.

Lastly, we express our opinion that solvent purity requires more attention in the field of monolayer self-assembly at liquid-solid interfaces, in particular for quantitative studies. Solvents are almost exclusively used as received, but our study unambiguously shows that even batch-to-batch variations can have a profound effect on kinetics, potentially further extending to thermodynamics. Detailed knowledge on the chemical identity of impurities and a deeper understanding of their influence would not only be invaluable for the field, but constitutes a necessary precondition to improve both the batch-to-batch and lab-to-lab reproducibility of quantitative results.

ASSOCIATED CONTENT

Supporting Information. Details of experiments and calculations; sublimation and dissolution enthalpy measurements; additional desorption traces alongside with corresponding UV-vis spectra of respective pure solvents; alternative analysis of desorption traces; results of MM calculations on monolayers, islands and bulk crystal

The following files are available free of charge.

Supporting Information.pdf

AUTHOR INFORMATION

Notes

The authors declare no competing financial interests.

ACKNOWLEDGMENT

O.O. acknowledges financial support by the Helmut-Fischer-Stiftung. N.M. acknowledges the use of high-performance computing resources at the University of Sheffield: Iceberg and Sol clusters.

REFERENCES

(1) Ochs, O.; Hocke, M.; Spitzer, S.; Heckl, W. M.; Martsinovich, N.; Lackinger, M., Origin of Solvent-Induced Polymorphism in Self-Assembly of Trimesic Acid Monolayers at Solid–Liquid Interfaces. *Chem. Mater.* **2020,** *32* (12), 5057-5065.

(2) Kampschulte, L.; Werblowsky, T. L.; Kishore, R. S. K.; Schmittel, M.; Heckl, W. M.; Lackinger, M., Thermodynamical Equilibrium of Binary Supramolecular Networks at the Liquid−Solid Interface. *J. Am. Chem. Soc.* **2008,** *130* (26), 8502-8507.

(3) Blunt, M. O.; Adisoejoso, J.; Tahara, K.; Katayama, K.; Van der Auweraer, M.; Tobe, Y.; De Feyter, S., Temperature-Induced Structural Phase Transitions in a Two-Dimensional Self-Assembled Network. *J. Am. Chem. Soc.* **2013,** *135* (32), 12068-12075.

(4) Li, M.; Xie, P.; Deng, K.; Yang, Y.-L.; Lei, S.-B.; Wei, Z.-Q.; Zeng, Q.-D.; Wang, C., A dynamic study of the structural change in the binary network in response to guest inclusion. *Phys. Chem. Chem. Phys.* **2014,** *16* (19), 8778-8782.

(5) Song, W.; Martsinovich, N.; Heckl, W. M.; Lackinger, M., Born–Haber Cycle for Monolayer Self-Assembly at the Liquid–Solid Interface: Assessing the Enthalpic Driving Force. *J. Am. Chem. Soc.* **2013,** *135* (39), 14854-14862.

(6) Song, W.; Martsinovich, N.; Heckl, W. M.; Lackinger, M., Thermodynamics of 4,4′-stilbenedicarboxylic acid monolayer self-assembly at the nonanoic acid–graphite interface. *Phys. Chem. Chem. Phys.* **2014,** *16* (26), 13239-13247.

(7) Bellec, A.; Arrigoni, C.; Schull, G.; Douillard, L.; Fiorini-Debuisschert, C.; Mathevet, F.; Kreher, D.; Attias, A.-J.; Charra, F., Solution-growth kinetics and thermodynamics of nanoporous self-assembled molecular monolayers. *J. Chem. Phys.* **2011,** *134* (12), 124702.

(8) Jahanbekam, A.; Chilukuri, B.; Mazur, U.; Hipps, K. W., Kinetically Trapped Two-Component Self-Assembled Adlayer. *J. Phys. Chem. C* **2015,** *119* (45), 25364-25376.

(9) Sirtl, T.; Song, W.; Eder, G.; Neogi, S.; Schmittel, M.; Heckl, W. M.; Lackinger, M., Solvent-dependent stabilization of metastable monolayer polymorphs at the liquid-solid interface. *ACS Nano* **2013,** *7* (8), 6711-8.

(10) Bhattarai, A.; Mazur, U.; Hipps, K. W., Desorption Kinetics and Activation Energy for Cobalt Octaethylporphyrin from Graphite at the Phenyloctane Solution–Graphite Interface: An STM Study. *J. Phys. Chem. C* **2015,** *119* (17), 9386-9394.

(11) Bhattarai, A.; Marchbanks-Owens, K.; Mazur, U.; Hipps, K. W., Influence of the Central Metal Ion on the Desorption Kinetics of a Porphyrin from the Solution/HOPG Interface. *J. Phys. Chem. C* **2016,** *120* (32), 18140-18150.

(12) Eder, G.; Kloft, S.; Martsinovich, N.; Mahata, K.; Schmittel, M.; Heckl, W. M.; Lackinger, M., Incorporation Dynamics of Molecular Guests into Two-Dimensional Supramolecular Host Networks at the Liquid–Solid Interface. *Langmuir* **2011,** *27* (22), 13563-13571.

(13) Kunitake, M.; Akiba, U.; Batina, N.; Itaya, K., Structures and Dynamic Formation Processes of Porphyrin Adlayers on Iodine-Modified Au(111) in Solution: In Situ STM Study. *Langmuir* **1997,** *13* (6), 1607-1615.

(14) Waldmann, T.; Klein, J.; Hoster, H. E.; Behm, R. J., Stabilization of Large Adsorbates by Rotational Entropy: A Time-Resolved Variable-Temperature STM Study. *Chemphyschem* **2013,** *14* (1), 162-169.

(15) Wen, R.; Rahn, B.; Magnussen, O. M., Potential-Dependent Adlayer Structure and Dynamics at the Ionic Liquid/Au(111) Interface: A Molecular-Scale In Situ Video-STM Study. *Angew. Chem. Int. Ed.* **2015,** *54* (20), 6062-6066.

(16) Gao, Y.; Olsen, K. W., Molecular Dynamics of Drug Crystal Dissolution: Simulation of Acetaminophen Form I in Water. *Mol. Pharm.* **2013,** *10* (3), 905-917.

(17) Elts, E.; Greiner, M.; Briesen, H., Predicting Dissolution Kinetics for Active Pharmaceutical Ingredients on the Basis of Their Molecular Structures. *Cryst. Growth Des.* **2016,** *16* (7), 4154-4164.

(18) Parks, C.; Koswara, A.; Tung, H.-H.; Nere, N. K.; Bordawekar, S.; Nagy, Z. K.; Ramkrishna, D., Nanocrystal Dissolution Kinetics and Solubility Increase Prediction from Molecular Dynamics: The Case of α-, β-, and γ-Glycine. *Mol. Pharm.* **2017,** *14* (4), 1023-1032.

(19) Liu, J. C.; Tan, E. L.; Chien, Y. W., Dissolution Kinetics and Rate-Controlling Mechanisms. *Drug Dev. Ind. Pharm.* **1986,** *12* (8-9), 1357-1370.

(20) Heininger, C.; Kampschulte, L.; Heckl, W. M.; Lackinger, M., Distinct differences in self-assembly of aromatic linear dicarboxylic acids. *Langmuir* **2009,** *25* (2), 968-72.

(21) Clair, S.; Pons, S.; Seitsonen, A. P.; Brune, H.; Kern, K.; Barth, J. V., STM Study of Terephthalic Acid Self-Assembly on Au(111): Hydrogen-Bonded Sheets on an Inhomogeneous Substrate. *J. Phys. Chem. B* **2004,** *108* (38), 14585-14590.

(22) Zhu, N.; Osada, T.; Komeda, T., Supramolecular assembly of biphenyl dicarboxylic acid on Au(111). *Surf Sci.* **2007,** *601* (8), 1789-1794.

(23) Ochs, O.; Heckl, W. M.; Lackinger, M., Immersion-scanning-tunneling-microscope for long-term variable-temperature experiments at liquid-solid interfaces. *Rev. Sci. Instrum.* **2018,** *89* (5), 053707.

(24) Gutzler, R.; Sirtl, T.; Dienstmaier, J. F.; Mahata, K.; Heckl, W. M.; Schmittel, M.; Lackinger, M., Reversible Phase Transitions in Self-Assembled Monolayers at the Liquid−Solid

Interface: Temperature-Controlled Opening and Closing of Nanopores. *J. Am. Chem. Soc.* **2010,** *132* (14), 5084-5090.

(25) Marie, C.; Silly, F.; Tortech, L.; Müllen, K.; Fichou, D., Tuning the Packing Density of 2D Supramolecular Self-Assemblies at the Solid−Liquid Interface Using Variable Temperature. *ACS Nano* **2010,** *4* (3), 1288-1292.

(26) Jahanbekam, A.; Vorpahl, S.; Mazur, U.; Hipps, K. W., Temperature Stability of Three Commensurate Surface Structures of Coronene Adsorbed on Au(111) from Heptanoic Acid in the 0 to 60 °C Range. *J. Phys. Chem. C* **2013,** *117* (6), 2914-2919.

(27) Giesen, M.; Baier, S., Atomic transport processes on electrodes in liquid environment. *J. Phys.: Condens. Matter* **2001,** *13* (21), 5009-5026.

(28) Jahanbekam, A.; Mazur, U.; Hipps, K. W., A new variable temperature solution-solid interface scanning tunneling microscope. *Rev. Sci. Instrum.* **2014,** *85* (10), 103701.

(29) Lackinger, M.; Griessl, S.; Markert, T.; Jamitzky, F.; Heckl, W. M., Self-Assembly of Benzene−Dicarboxylic Acid Isomers at the Liquid Solid Interface: Steric Aspects of Hydrogen Bonding. *J. Phys. Chem. B* **2004,** *108* (36), 13652-13655.

(30) Xiao, W. D.; Jiang, Y. H.; Aït-Mansour, K.; Ruffieux, P.; Gao, H. J.; Fasel, R., Chiral Biphenyldicarboxylic Acid Networks Stabilized by Hydrogen Bonding. *J. Phys. Chem. C* **2010,** *114* (14), 6646-6649.

(31) Stepanow, S.; Lin, N.; Vidal, F.; Landa, A.; Ruben, M.; Barth, J. V.; Kern, K., Programming Supramolecular Assembly and Chirality in Two-Dimensional Dicarboxylate Networks on a Cu(100) Surface. *Nano Lett.* **2005,** *5* (5), 901-904.

(32) Cortés, R.; Mascaraque, A.; Schmidt-Weber, P.; Dil, H.; Kampen, T. U.; Horn, K., Coexistence of Racemic and Homochiral Two-Dimensional Lattices Formed by a Prochiral Molecule: Dicarboxystilbene on Cu(110). *Nano Lett.* **2008,** *8* (12), 4162-4167.

(33) Desiraju, G.; Steiner, T., *The Weak Hydrogen Bond: In Structural Chemistry and Biology*. Oxford University Press: 2001, DOI:10.1093/acprof:oso/9780198509707.001.0001, p 507.

(34) Baber, A. E.; Tierney, H. L.; Sykes, E. C. H., A Quantitative Single-Molecule Study of Thioether Molecular Rotors. *ACS Nano* **2008,** *2* (11), 2385-2391.

(35) Kumagai, T.; Hanke, F.; Gawinkowski, S.; Sharp, J.; Kotsis, K.; Waluk, J.; Persson, M.; Grill, L., Thermally and Vibrationally Induced Tautomerization of Single Porphycene Molecules on a Cu(110) Surface. *Phys. Rev. Lett.* **2013,** *111* (24), 246101.

(36) Marbach, H.; Steinrück, H. P., Studying the dynamic behaviour of porphyrins as prototype functional molecules by scanning tunnelling microscopy close to room temperature. *Chem. Commun.* **2014,** *50* (65), 9034-9048.

(37) Bhattarai, A.; Mazur, U.; Hipps, K. W., A Single Molecule Level Study of the Temperature-Dependent Kinetics for the Formation of Metal Porphyrin Monolayers on Au(111) from Solution. *J. Am. Chem. Soc.* **2014,** *136* (5), 2142-2148.

(38) Jung, L. S.; Campbell, C. T., Sticking Probabilities in Adsorption of Alkanethiols from Liquid Ethanol Solution onto Gold. *J. Phys. Chem. B* **2000,** *104* (47), 11168-11178.

(39) Hipps, K. W.; Mazur, U., Kinetic and Thermodynamic Control in Porphyrin and Phthalocyanine Self-Assembled Monolayers. *Langmuir* **2018,** *34* (1), 3-17.

(40) Martsinovich, N.; Troisi, A., Modeling the Self-Assembly of Benzenedicarboxylic Acids Using Monte Carlo and Molecular Dynamics Simulations. *J. Phys. Chem. C* **2010,** *114* (10), 4376-4388.

(41) Miliordos, E.; Xantheas, S. S., On the validity of the basis set superposition error and complete basis set limit extrapolations for the binding energy of the formic acid dimer. *J. Chem. Phys.* **2015,** *142* (9), 094311.

(42) Lackinger, M.; Griessl, S.; Kampschulte, L.; Jamitzky, F.; Heckl, W. M., Dynamics of Grain Boundaries in Two-Dimensional Hydrogen-Bonded Molecular Networks. *Small* **2005,** *1* (5), 532-539.

(43) Rossignol, S.; Tinel, L.; Bianco, A.; Passananti, M.; Brigante, M.; Donaldson, D. J.; George, C., Atmospheric photochemistry at a fatty acid–coated air-water interface. *Science* **2016,** *353* (6300), 699.